JACS Au
AN OPEN ACCESS JOURNAL OF THE AMERICAN CHEMICAL SOCIETY

pubs.acs.org/jacsau
Article

T7 Endonuclease I-Mediated Single-Base Mismatch Biosensing Strategy for High-Resolution Quantitative Analysis of 5-Hydroxymethylcytosine in Genomic DNA

Zhihan Zhao, Shixing Chen, Zhixiao Liu, Jing Su, Junhong Lü, Lihong Hao, Yanzhi Dou,* Lihua Wang,* and Shiping Song*

Cite This: JACS Au 2025, 5, 1320−1327
Read Online

ACCESS | Metrics & More | Article Recommendations | Supporting Information

ABSTRACT: 5-hydroxymethylcytosine (5hmC) plays a pivotal role in the DNA demethylation pathway and transcriptional regulation. While sequencing-based methods such as TET-assisted bisulfite sequencing offer single-base resolution, they are not ideal for dynamic, time-sensitive quantification. Here, we present a novel enzymatic biosensing strategy leveraging T7 endonuclease I for rapid and locus-specific 5hmC detection with a single-base resolution. This electrochemical platform captures double-tagged dsDNA and detects 5hmC by monitoring the signal reduction upon T7 endonuclease cleavage of A-C mismatches. The method achieved high sensitivity, detecting as little as 10 pg of hydroxymethylated DNA amid a 100,000-fold excess of methylated or unmethylated DNA. Furthermore, we demonstrated its ability to quantify real-time 5hmC variation during umbilical cord mesenchymal stem cell differentiation. This approach offers a powerful tool for 5hmC analysis in dynamic biological processes.

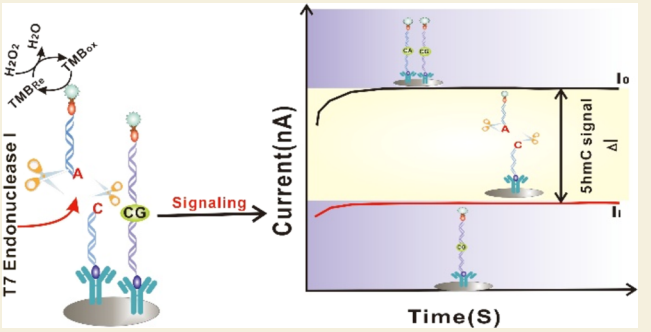

KEYWORDS: *5hmC, high-resolution quantitation, biosensing, T7 endonuclease I, UC-MSCs*

INTRODUCTION

5-Hydroxymethylcytosine (5hmC) is oxidized from 5-methylcytosine (5mC) in a Fe^{2+}- and 2-oxoglutarate-dependent manner by 10-11 translocation (TET) family protein.[1,2] 5hmC has been proposed as an intermediate in the demethylation pathway,[3,4] and its uneven distribution across different tissues suggests that it plays a role in gene regulation.[5−7] Moreover, reserach on 5hmC and TET protein demonstrated that 5hmC was closely related to brain development,[8−11] zygote development,[9] and embryonic stem cells maintenance.[12−15] Especially, the enrichment of TET and 5hmC at gene promoters indicates that TET-mediated hydroxymethylation may be involved in transcriptional regulation.[16,17] The depletion of TET results in a reduced expression of a set of genes, including pluripotency-related factors like Nanog, Esrrb, and Tcl1, providing further evidence that TeT and 5hmC directly contribute to the transcription of specific pluripotency genes.[18−22]

Methods for detecting 5hmC can generally be categorized based on their genomic resolution. Techniques to quantify the global levels of 5hmC include thin layer chromatography,[23] high-performance liquid chromatography,[24] and liquid chromatography−mass spectrometry.[25,26] However, only providing average 5hmC levels across the entire genome is limited to detecting large-scale changes. Methods based on DNA immunoprecipitation were developed to measure the enrichment of 5hmC content on locus-specific levels by 5hmC-specific antibody or the antibody specifically against the modified 5hmC.[27,28] While, these regional measures allow for locus-specific analysis, they do not quantify 5hmC at individual CpG sites, limiting their ability to study the impact of environmental factors on specific CpG sites. Methods for base-pair-resolution detection can quantify 5hmC at individual CpG sites in the genome, which can be linked to genes for downstream pathway analysis and mechanistic studies. Currently, widely used methods to measure base-pair level 5hmC are bisulfite sequencing and its derived methods including TET-assisted bisulfite sequencing (TAB-seq)[29] and oxidative bisulfite sequencing(oxBS).[30] Although these sequencing-based strategies can achieve good performance, they are also labor-intensive and time-consuming (at least 2 weeks totally). Here, we developed a simple and rapid locus-specific 5hmC strategy (within 24 h), which can identify 5hmC at a single-base resolution. In this strategy, we used T7

Received: December 5, 2024
Revised: January 15, 2025
Accepted: January 16, 2025
Published: February 17, 2025

Endonuclease I, which could sensitively distinguish and cleave A-C mismatch generated by the hybridization of oxidative bisulfite (Oxbis)-treated DNA and bisulfite (Bis)-treated DNA. Notably, this strategy could test 10 pg of hydroxymethylated DNA, even in the presence of a 100,000-fold excess of methylated or unmethylated DNA. Then, we achieved real-time quantification of 5hmC variation in the context of umbilical cord mesenchymal stem cells (UC-MSCs) differentiation, which sequencing-based methods were not suitable for. Several lines of evidence suggested that 5hmC plays a crucial role in the establishment and/or maintenance of a pluripotency during early embryonic development. We anticipate that the proposed quantification method will help further uncover the roles of 5hmC in early development and cellular homeostasis.

METHODS

Construction of 5hmC-Containing DNA Strand Based on pBR322

In 50 μL of PCR reaction, 1 μg of pBR322 (0.5 μg/μL), 5 μL of 10× PCR Buffer, 4 μL of dNTP(2.5 nM), 0.5 μLTakaRaTaq, 2 μL of primer1-Fw (10 μM), 2 μL of primer1-Rv (10 μM), and Milli-Q water were mixed. The reaction was first heated to 95 °C for 3 min, followed by 35 cycles of 30 s at 95 °C, 30 s at 56 °C, and 30 s at 72 °C, with a final extension cycle of 72 °C for 5 min. Then, we took 30 μL of PCR product mixed with 10 μL of MilliQ water, 5 μL of Lambda buffer, and 5 μL of Lambda exonuclease in 37 °C for 2 h following 75 °C incubation for 10 min. After this, the samples were purified and concentrated to 20 μL of MilliQ with a TakaRa Mini BEST DNA Fragment Purification Kit Ver.4.0. Then, the extension process went as follows: 20 μL of purified PCR product, 10 μL of extension primer(10 μM), 5 μL of 10× Buffer, 1.2 μL of VentR DNA enzyme, 1 μL of dCTP/dGTP mix, and 13.8 μL of Milli-Q water were mixed together under the condition of 95 °C for 5 min, followed by 8 cycles of 5 s at 80 °C, 1 min at 55 °C, and 30 s at 72 °C, with a final extension cycle of 72 °C for 1 min. The 50 μL extension product was purified with the same kit and concentrated into 20 μL of MilliQ. Then, the 20 μL purified sample, 4 μL of dNTP (2.5 mM), 5 μL of 10× Buffer, 1.2 μL of VentR DNA enzyme, and 19.8 μL of MilliQ were mixed together under the condition of 55 °C for 2 min, followed by 72 °C for 40 min. The supplemental reaction was concentrated to 16 μL of MilliQ with the purification kit. Finally, 16 μL of purified sample, 2 μL of *Hha*I endonuclease, and 2 μL of 10 × Buffer were mixed together under 37 °C for 30 min and loaded onto 2% agrose gel.

T7 Endonuclease I Cleavage

We annealed two single strand DNA that including different kinds of mismatch types (A-C, G-T, AA-CC, GG-TT, ANA-CNC, GNG-TNT) with hybridization buffer (1.2 M NaCl, 12 mM Tris-HCl, 14 mM $MgCl_2$) followed by annealing from 95 to 25 °C in 2 h in the Applied Biosystems. Then, 500 mg of annealed dsDNA was incubated with 5 μL T7 endonuclease I and 5 μL T7 reaction buffer in 50 μL reaction under 37 °C for 16 h.

Oxidation and Sodium-Bisulfite Treatment

We referred to Michael J. Booth's protocol for the oxidation. 1 μg DNA was denatured in 0.05 M NaOH (totally volume 19 μL) for 30 min at 37 °C and then snap-cooled on ice for 5 min. After that, 1 μL of KRuO4 solution (15 mM KRuO4 in 0.05 M NaOH) was added, and the reaction was maintained on ice for 1 h with occasional vortexing. Then the second round 1 μL KRuO4 solution was added and held on ice for 1 h with occasional vortex. Finally, we used MilliQ water to supplement to 50 μL and purified with the mini quick spin oligo columns following the protocol. The sodium-bisulfite modification was done as follows. 1 μg DNA was dissolved in 50 μL of distilled water denatured for 20 min at 95 °C and further denatured in 0.3 M NaOH for 15 min at 45 °C. Subsequently, 520 μL of a 3.6 M sodium bisulfite solution (pH 5.0) containing 10 mM hydroquinone was added, and the reaction was incubated at 55 °C for 16 h in the dark to avoid oxidation. The modified DNA was then desalted with Wizard Plus Minipreps DNA Purification System (Promega) and then was dissolved in 50 μL of 1 mmol/L Tris-HCl (pH 8.0). Then desulfonation was done by adding 0.3 mol/L NaOH with 40 °C for 15 min, followed by neutralization with 50 μL of 3 M ammonium acetate and the addition of 1 μL of glycogen (20 mg/L). After precipitation with 70% ethanol overnight, the DNA was resuspended in 30 μL of 1 mM Tris-HCl (pH 8.0). For oxidation bisulfite treatment, we did oxidation first, and then we did sodium-bisulfite modification.

UCMS Cells Culture, Differentiation, and Oil Red-O Staining

The UCMS cells were cultured in Dulbecco's modified Eagle's medium (Gibo), supplemented with 10% fetal calf serum and 1% penicillin/streptomycin. Cells were grown at 37 °C in a humidified atmosphere with 5% (v/v) CO_2. Cells were plated in a 60 mm dish and cultured until 80% confluence was reached in complete culture medium. Then, the medium was replaced with adipogenic medium (complete culture medium supplemented with 50 μM in domethacin, 0.5 mM isobutylmethylxanthine, and 0.5 μM dexamethasone), kept culturing for 14 days with adipogenic medium, and changed the medium every 2 days. Differentiated stem cells were fixed in 10% formalin for 10 min, washed with 60% isopropanol 20−30 s, and stained with Oil Red-O staining solution for 10−15 min. After washing twice with 60% isopropanol for 20s each, the cells were washed with distilled water and air-dried at room temperature.

Methylation of Genomic DNA

Genomic DNA were prepared using a Cultured Cell DNA Extraction Kit. Then we mixed 1 μg DNA sample, 1 μL SAM, 5 μL NEB buffer, and 1 μL CpG transmethylaseM. SssI enzyme under the condition of 37 °C for 3 h.

Fabrication of the Multiplexing Electrochemical Biosensor (MEB)

The electrochemical performance of the MEB was assessed by cyclic voltammetry (CV) and amperometric methods using a custom-built 16-channel electrochemical detector. CV measurements were performed over 2 segments, with a potential window of −0.3−0.6 V, and amperometric measurements were taken at −0.05 V for 100 s. Prior to assembling the antidigoxin antibody, the screen-printed carbon electrode (SPCE) was electrochemically activated to generate carboxylate groups. The CV scan of SPCE in 0.01 M phosphate buffer (pH 7.2) was run for 30 cycles, with a potential range of −0.3 to 0.6 V at a scan rate of 500 mV/s. The electrodes were then coated with a 10 μL mixture of 76.65 mg/mL ethylhydroxyethylcellulose (EH) and 11.05 mg/mL *N*-hydroxysuccinimide (NHS) for 15 min to activate the carboxylate groups. Then, 8 μL of antidigoxin antibody (3 μg/mL) was incubated on the carbon electrode. The electrodes were washed with 0.01 M PBS and blocked with 1% Casein. After this, only digoxin-modified DNA samples were captured, following 1 h of incubation on the electrode. After washing 3 times, 10 μL of streptavidin-horseradish peroxidase (SA-HRP) (1:1000 dilution in 1% Casein) was added and incubated at 37 °C for 40 min, followed by five washes with 0.01 M PBS. Finally, only the both biotin-modified and digoxin-modified DNA samples stayed on the electrode. TMB substrate (50 μL) was then added, and the reaction was simultaneously detected across all 16 channels using CV measurement at a scan rate of 0.1 V/s with the potential range of −0.3 to 0.6 V. The amperometric measurement was performed at −0.05 V, and the electrochemical reduction current was recorded 100 s after the SA-HRP redox reaction reached steady state.

https://doi.org/10.1021/jacsau.4c01184
JACS Au 2025, 5, 1320−1327

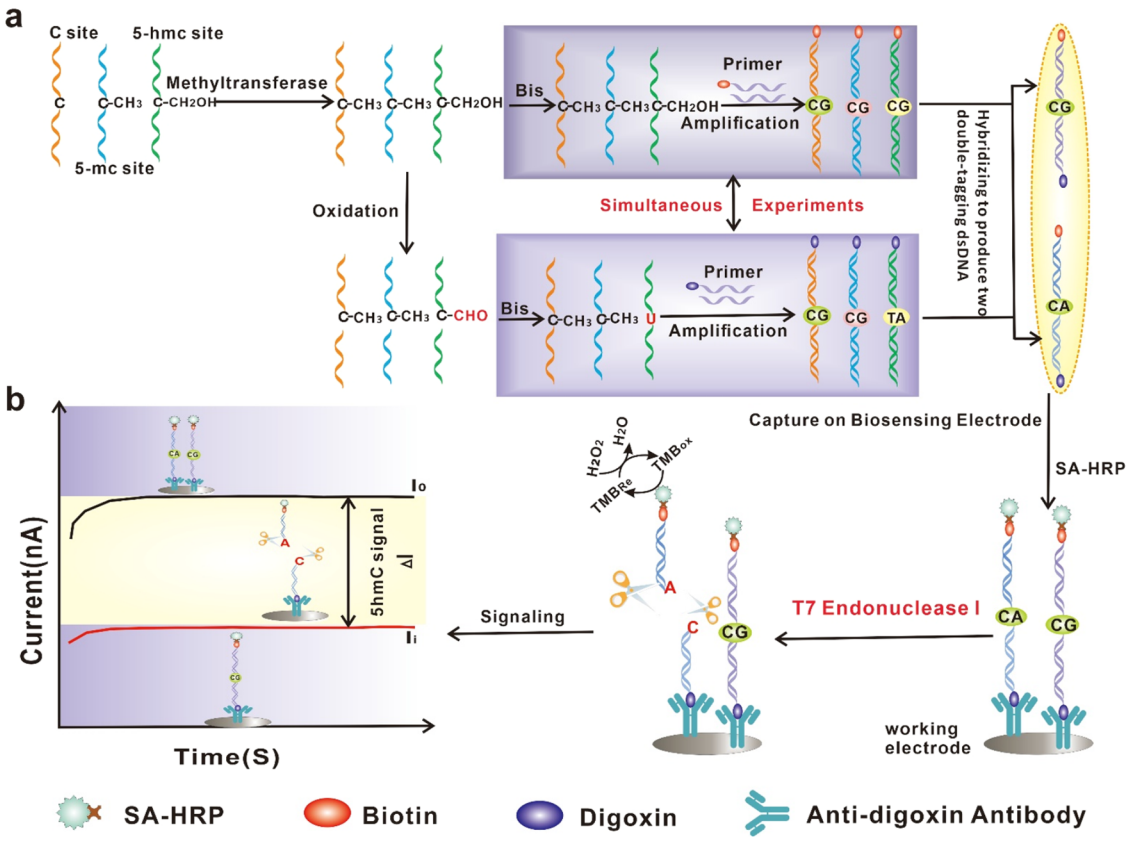

Figure 1. Principle of quantitative analysis of 5-hmC based on the T7 Endonuclease I-mediated single-base mismatch biosensing strategy. (a) Methyltransferase converts cytosine (C) into 5-methylcytosin (5-mC), pursued by simultaneous bisulfite and oxidative bisulfite treatments. Specific primer are then applied, resulting in two types of double-tagged dsDNA. (b) Detection process on a biosensing electrode involves biotin-digoxin labeling and SA-HRP-based signaling. T7 endonuclease I selectively cleaves the target DNA at mismatched 5-hmC sites, allowing signal quantification based on current changes. The curve represents the electrochemical signal associated with the presence of 5-hmC

RESULTS AND DISCUSSION

T7 Endonuclease I-Mediated Single-Base Mismatch Strategy to Quantify 5-Hydroxymethylcytosine

The new strategy was based on two parallel processes for Bis/Oxbis treatment, DNA amplification and T7 endonuclease I-mediated single-base mismatch recognition biosensing (Figure 1). The first step was to use CpG methyltransferase to methylate C/5mC/5hmC, where C was transferred to 5mC while 5mC and 5hmC remained unchanged. Then, the treated DNAs were applied to Bis treatment and Oxbis treatment separately. After Bis treatment and amplification (Bis-Fw1/Rv1), both 5mC and 5hmC were read as C, and the C-containing DNA strand was tagged with biotin. Meantime, after Oxbis treatment, 5mC was read as C, whereas 5hmC was first oxidized to 5fC, then converted to U and read as T. Afterward, DNA strands containing C or T were labeled with digoxigenin after PCR amplification (Oxbis-Fw1/Rv1). Subsequently, hybridization between two groups (the Bis and the Oxbis treatment) resulted in six kinds of dsDNA: biotin C-G digoxigenin, biotin C-A digoxigenin, biotin C-G, C-G digoxigenin, C-G, and T-G. Among them, only two dual-labeled dsDNA could be captured on the biosensing electrode and showed current signals following the incubation of SA-HRP. Then T7 Endonuclease I was introduced to recognize and cleave mismatched DNA (A-C), contributing to the current signal reduction. Because the A-C mismatch was originated from 5hmC, its amount was positively correlated with the current difference.

Exploring the Detection Sensitivity of 5hmC in C-Containing and 5mC-Containing DNA Strands In Vitro

To investigate the sensitivity of this strategy, we first established the 5hmC-containing DNA strand (Figure S1) and diluted it with different ratios in the context of 5mC-containing DNA strand and C-containing DNA strand separately. Then, the lowest ratio we can detect was 1/100,000 in both the 5mC- containing DNA strand and the C-containing DNA strand (Figure 2). We summarized this high sensitivity for several factors. First, the semilabeled primer amplication strategy ensures that only double-labeled dsDNA can be captured on the biosensing electrode, excluding the semilabeled or nonlabeled dsDNA, and improves the signal-to-noise ratio. Second, the electrochemical platform, this signal transducer, could directly quantify electrochemical reaction on the electrode and provides a strong and sensitive signal. Third, T7 Endonuclease I was very sensitive to recognize and cleave the A-C mismatch and was compatible with the biosensing platform. Fourth, the high Bis and Oxbis treatment efficiency achieves a high base conversion rate, attributing the maximum amount of mismatch DNA.

Optimizing the T7 Endonuclease I Cleavage and Oxbis Treatment

T7 Endonuclease I is a stable homodimer comprising two catalytic domains connected by a bridge,[31] which can realize

https://doi.org/10.1021/jacsau.4c01184
JACS Au 2025, 5, 1320−1327

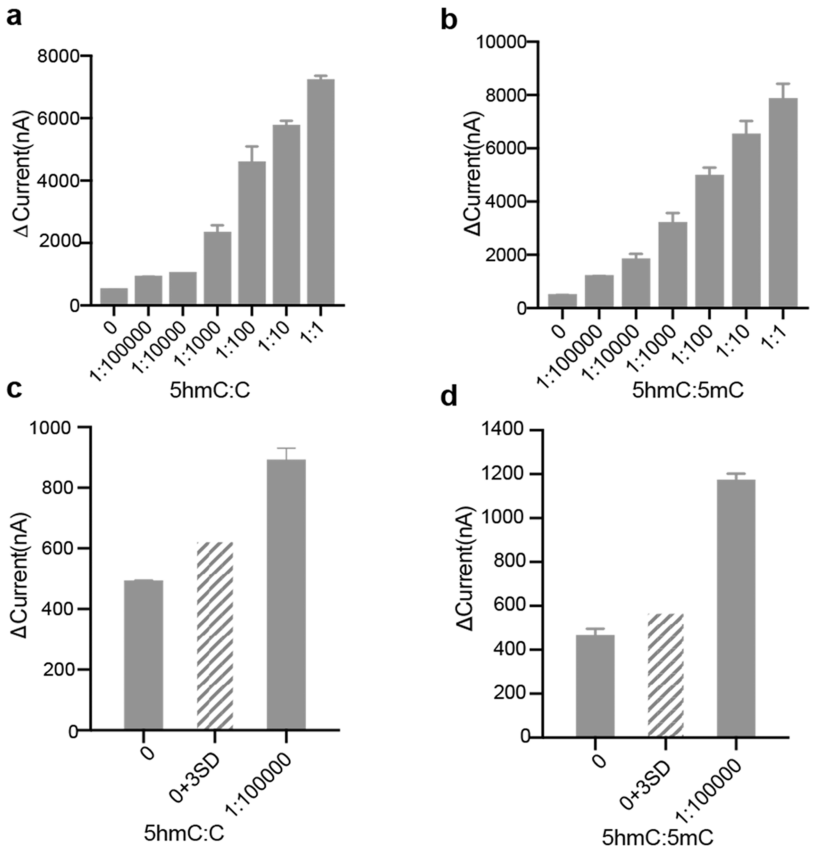

Figure 2. Quantitative evaluation of 5hmC in C-containing and 5mC-containing DNA strands. (a) Response current to 5hmC:C at a serious ratio. (b) Response current to 5hmC:5mC at a serious ratio. (c) Sensitivity of the proposed 5hmC detection strategy in the 5mC-containing DNA strand. The dashed lines represent the blank value plus three times the standard deviations. (d) Sensitivity of the proposed 5hmC detection strategy in the C-containing DNA strand. The dashed lines indicate the blank value plus three times standard deviations. Error bars represent standard deviations of three independent measurements.

base-pair mismatch cleavage in dsDNA, especially the C-containing mismatch. Hence, T7 Endonuclease I has been widely used in mutation detection[32] and single nucleotide polymorphism.[33] We compared T7 Endonuclease I with different base-pair mismatch recognition enzymes such as TDG enzyme, Endonuclease V, and Taq Muts. As we can see in Figure S2, T7 Endonuclease I is the best at identifying AA-CC and ACA-CGC mismatch types, which is more in line with our strategy. Also, we tried to improve the enzyme's catalytic performance by optimizing its reaction condition including temperature, incubation time, and Mg^{2+}concentration. We found that T7 Endonuclease I has better performance at 37 °C, 6−16 h, and 1 mM Mg^{2+} (Figure 3a). Interestingly, the Mg^{2+} concentration of the commercial reaction buffer for T7 endonuclease I is 1.0 mM, but we found that a lower Mg^{2+} concentration has better cleavage efficiency, which we think higher Mg^{2+} concentration may increase the distance between the two catalytic centers, thereby reducing the cleavage efficiency. Finally, we investigated the compatibility of T7 Endonuclease I cleavage with our biosensing platform for six different mismatch types. A-C mismatch could induce more than 5000 nA current difference, which proved the feasibility of this strategy (Figure 3b).

The efficiency of the Oxbis treatment was another key parameter in our design. The oxidation bisulfite efficiency evaluation was based on *Hha* I endonuclease to cleave the symmetric sequence 5 -GCG ↓C-3′ in dsDNA. *Hha* I endonuclease would not work when the "C" changed to "T" after Oxbis treatment (Figure 3c). We investigated the reaction pH and the amount of $KRuO_4$. By selecting optimized conditions (pH of 9 and 0.9 mM $KRuO_4$), we found the oxidative bisulfite efficiency was around 60% (Figure 3c). However, we, when the Oxbis efficiency increased up to 90% (Figure 3c), completely removed the ethanol by incubating the reaction, demonstrating that ethanol was the key factor that inhibits the solution for 30 min at room temperature before Oxbis treatment, oxidative bisulfite efficiency.

Tracking the Dynamic Changes of 5hmC in UC-MSCs

UC-MSCs, derived from the extraembryonic mesoderm, have been extensively studied for their ability to differentiate into adipogenic, chondrogenic, and osteogenic lineages. Our primary human mesenchymal stem cells were obtained from the Medical College of Shandong University. UC-MSCs are a versatile cell population found in various tissues, capable of differentiating into multiple lineages.[34] During its differentiation into adipose cells, TET1 can directly bind to the promoter of the insulin-like growth factor 2 mRNA binding protein 1 (IGF2BP1) and affect its hydroxymethylation status.[16] By tracking the dynamic changes of 5hmC during differentiation, we gain valuable insights into the epigenetic regulation of gene expression.

As shown in Figure 4a, cells were harvested on days 1, 2, 7, and 14. Oil Red-O positive cells appeared on day 7, and the number of adipocytes increased by day 14, confirming the successful adipogenic induction. In parallel, cells were

https://doi.org/10.1021/jacsau.4c01184
JACS Au 2025, 5, 1320−1327

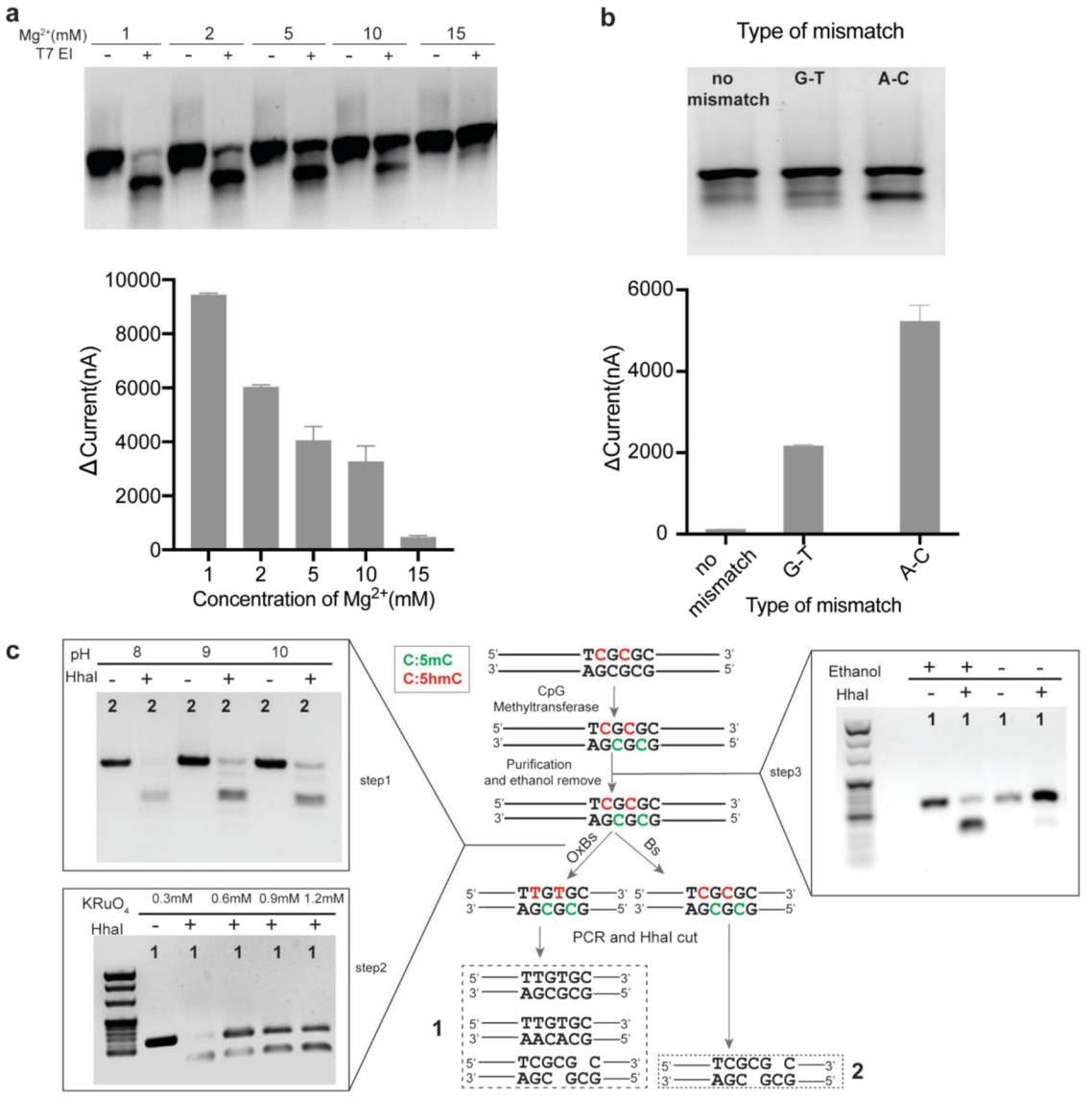

Figure 3. Optimization of T7 endonuclease I cleavage and Oxbis bisulfite treatment. (a) Agarose gel electrophoresis and electrochemical data showing the effect of Mg^{2+} concentration on the cleavage performance of T7 endonuclease I, with optimal activity observed at 1 mM Mg^{2+}. (b) Agarose gel electrophoresis and electrochemical data showing the cleavage performance of T7 endonuclease I for two mismatch types (G-T and A-C), with higher ΔCurrent values observed for A−C mismatches. (c) Factors influencing Oxbis treatment. Step 1: Optimization of reaction pH, with pH 9 showed the best results. Step 2: Evaluation of $KRuO_4$ concentration on DNA cleavage indicated optimal efficiency at 0.9 mM. Step 3: Assessment of ethanol treatment prior to bisulfite and oxidative bisulfite treatments.

harvested at corresponding time points to extract the genome DNA and do PCR based on IGF2BP1 promoter. Then, the PCR product was treated with CpG methyltransferase to prepare for our strategy. We can see the current value difference increased on the seventh day and then decreased on the 14th day, which indicated the changing trend of the 5hmC amount (Figure 4b). For DNA sequencing, the amount of framed T with Oxbis treatment could reflect the amount of 5hmC (Figure 4c). We barely saw 5hmC on day 1, the highest amount of 5hmC on day 7, and the decreased amount of 5hmC on day 14 (Figure 4c). Obviously, compared to Sanger DNA sequencing, which could only see 5hmC qualitatively, our biosensing strategy could dynamically quantify 5hmC. Overall, the state of stem cell differentiation process can be shown by monitoring the hydroxymethylation level, and the high and low hydroxymethylation level indicates that the UC-MSCs cell differentiation ability is reduced.

CONCLUSIONS

In this study, we proposed a rapid and inexpensive 5hmC quantitative biosensing analysis strategy, combining Bis/Oxbis treatment and the T7 Endonuclease I. It can detect 5hmC at single-base resolution with 10 pg of 5hmC in the presence of a 100,000-fold excess of 5mC or unmethylated C. We demonstrated the utility of this method to track the dynamic changes of 5hmC in gene IGF2BP1 during the UC-MSCs differentiation. This technique surpasses previous 5hmC identification methods by offering single-base resolution without the need for specialized equipment, making it suitable for various sequencing analysis. It represents a significant advancement in the comprehensive site-point analysis of 5hmC in both normal and abnormal cell differentiation. Aberrant DNA hyperventilation is linked to various diseases, including cancer; this method holds great potential. However, this method is currently limited by its inability to simultaneously

https://doi.org/10.1021/jacsau.4c01184
JACS Au 2025, 5, 1320−1327

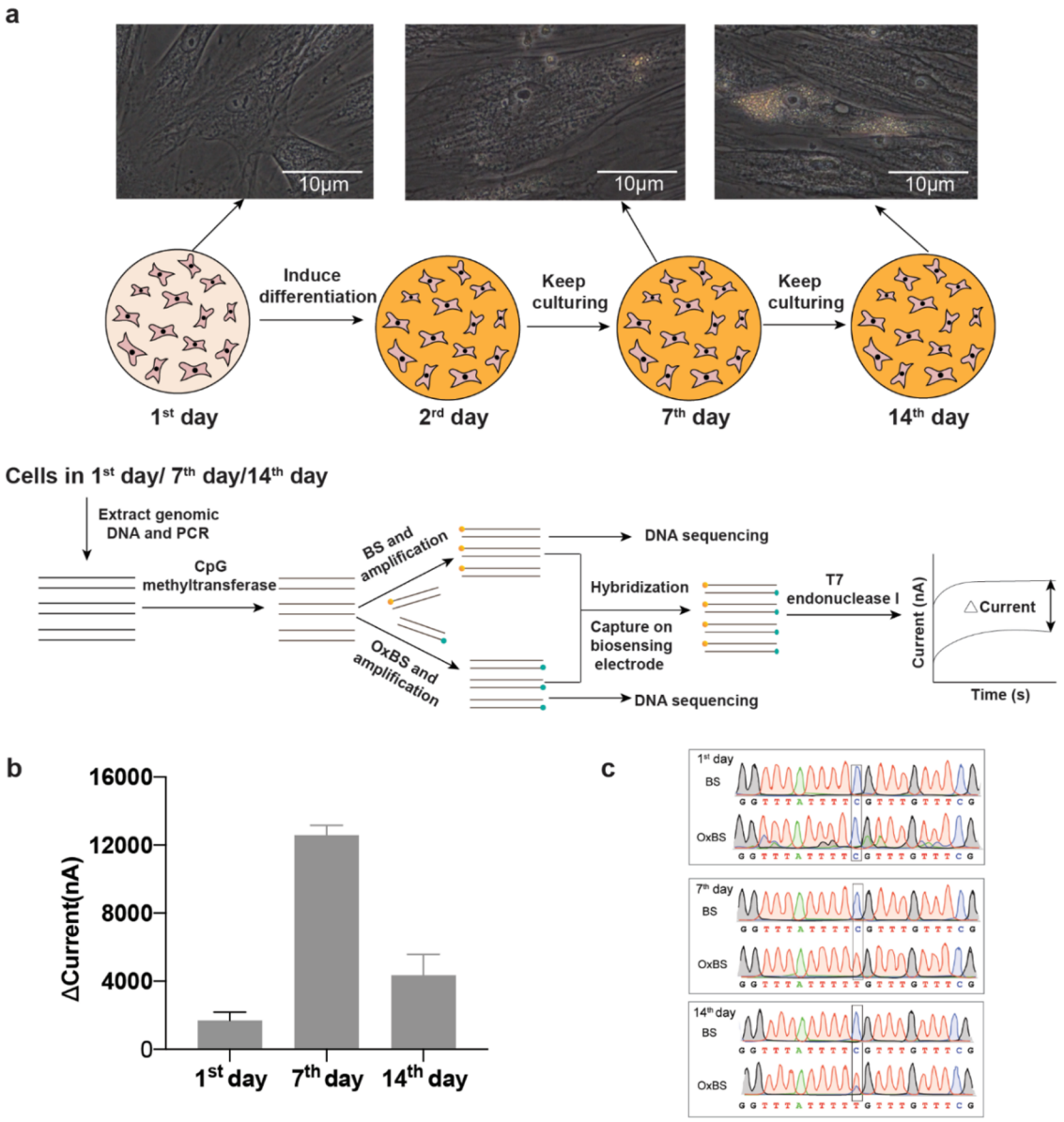

Figure 4. Application in UC-MSCs cells. (a) Schematic workflow of the 5hmC quantification during UC-MSCs cells differentiating toward the adipose cells. The cells were stained with Oil Red-O, a neutral lipid dye, at various time points during adipogenic differentiation (left). On the right, 5hmC quantification was performed using T7 Endonuclease I-mediated single-base mismatch strategy. (b) T7 Endonuclease I-mediated single-base mismatch biosensing strategy to quantify 5hmC during the differentiation of UC-MSCs cells. (c) Sanger sequencing of the PCR product based on genomic DNA with BS and OxBS treatment during the differentiation of UC-MSCs cells.

distinguish C, 5mC, and 5hmC, and its sensitivity is influenced by the sequence context. These limitations highlight areas for further exploration. Future research should prioritize improving the scalability of the biosensing method to enable high-throughput applications, such as multisample parallel analysis or seamless integration with automated systems. Additionally, expanding the method's capacity to detect other epigenetic modifications, such as 5-formylcytosine (5fC) and 5-carboxylcytosine (5caC), would enhance its utility for comprehensive epigenetic studies. Optimizing enzyme reaction conditions to mitigate environmental influences and developing alternative signal transduction mechanisms could further increase the robustness and adaptability of the platform. These advancements would not only address current limitations but also broaden the method's applicability in future epigenomic research.

■ ASSOCIATED CONTENT

Supporting Information

The Supporting Information is available free of charge at https://pubs.acs.org/doi/10.1021/jacsau.4c01184.

Materials and chemicals, design and synthesis of 5hmC-containing dsDNA, comparison of different enzymes under different mismatch type, optimization of T7 endonuclease I, and Oligos (PDF)

■ AUTHOR INFORMATION

Corresponding Authors

Yanzhi Dou − *Shanghai Institute of Applied Physics, Chinese Academy of Sciences, Shanghai 201800, China; Science and Technology on Microsystem Laboratory, Shanghai Institute of Microsystem and Information Technology Chinese Academy*

https://doi.org/10.1021/jacsau.4c01184
JACS Au 2025, 5, 1320−1327

of Science, Shanghai 200050, China; Email: douyanzhi@mail.sim.ac.cn

Lihua Wang − *Institute of Materiobiology, College of Science, Shanghai University, Shanghai 200444, China*; orcid.org/0000-0002-6198-7561; Email: wanglihua@shu.edu.cn

Shiping Song − *Institute of Materiobiology, College of Science, Shanghai University, Shanghai 200444, China; Shanghai Institute of Applied Physics, Chinese Academy of Sciences, Shanghai 201800, China*; orcid.org/0000-0002-0791-8012; Email: spsong@shu.edu.cn

Authors

Zhihan Zhao − *Institute of Materiobiology, College of Science, Shanghai University, Shanghai 200444, China; Shanghai Institute of Applied Physics, Chinese Academy of Sciences, Shanghai 201800, China*

Shixing Chen − *Shanghai Institute of Applied Physics, Chinese Academy of Sciences, Shanghai 201800, China*

Zhixiao Liu − *Department of Histology and Embryology, Naval Medical University, Shanghai 200433, China*

Jing Su − *Shanghai Institute of Applied Physics, Chinese Academy of Sciences, Shanghai 201800, China*

Junhong Lü − *School of Pharmacy, Binzhou Medical University, Yantai 264003, China*; orcid.org/0000-0003-2873-3137

Lihong Hao − *Ningbo Junkang Medical Technology Co., Ltd., Ningbo 315000, China*

Complete contact information is available at: https://pubs.acs.org/10.1021/jacsau.4c01184

Author Contributions

Z.Z. and S.C. designed and performed all experiments, interpreted the results, and wrote the manuscript. Z.L., J.L., and L.H. helped to set up and execute UC-MSCs differentiation and staining. Z.Z. and J.S. performed data analysis. D.Y. and L.W. worked with result discussion and the manuscript editing. S.S. conceived and directed the project, interpreted the results, and revised the manuscript.

Notes

The authors declare no competing financial interest.

■ ACKNOWLEDGMENTS

This work was supported by the National Key Research and Development Program of China (2023YFB3208200) and National Natural Science foundation of China (21974147).

■ ABBREVIATIONS

7−5hmC, 5-hydroxymethylcytosine; 5mC, 5-methylcytosine; TET, 10-11 translocation TET; Oxbis, oxidative bisulfite; Bis, bisulfite; UC-MSCs, umbilical cord mesenchymal stem cells

■ REFERENCES

(1) Tahiliani, M.; Koh, K. P.; Shen, Y. H.; Pastor, W. A.; Bandukwala, H.; Brudno, Y.; Agarwal, S.; Iyer, L. M.; Liu, D. R.; Aravind, L.; Rao, A. Conversion of 5-Methylcytosine to 5-Hydroxymethylcytosine in Mammalian DNA by MLL Partner TET1. *Science* **2009**, *324* (5929), 930−935.

(2) Xu, Z.; Wang, Z.; Hu, D.; Chen, H.; Yan, Y.; Li, Y.; Tu, M.; Shen, Q.; Liu, X.; Li, R.; et al. MXene Boosted Ultrasensitive Electrochemical Detection of 5-Hydroxymethylcytosine in Genomic DNA from Complex Backgrounds. *Adv. Funct. Mater.* **2024**, *34* (19), No. 2313118.

(3) Hahn, M. A.; Szabó, P. E.; Pfeifer, G. P. 5-Hydroxymethylcytosine: a stable or transient DNA modification? *Genomics* **2014**, *104* (5), 314−323.

(4) Li, C.-c.; Dong, Y.-h.; Zou, X.; Luo, X.; Shen, D.; Hu, J.; Zhang, C.-y. Label-Free and Template-Free Chemiluminescent Biosensor for Sensitive Detection of 5-Hydroxymethylcytosine in Genomic DNA. *Anal. Chem.* **2021**, *93* (4), 1939−1943.

(5) Nestor, C. E.; Ottaviano, R.; Reddington, J.; Sproul, D.; Reinhardt, D.; Dunican, D.; Katz, E.; Dixon, J. M.; Harrison, D. J.; Meehan, R. R. Tissue type is a major modifier of the 5-hydroxymethylcytosine content of human genes. *Genome Res.* **2012**, *22* (3), 467−477.

(6) Globisch, D.; Minzel, M.; Miller, M.; Michalakis, S.; Wagner, M.; Koch, S.; Brickl, T.; Biel, M.; Carell, T. Tissue distribution of 5-Hydroxymethyl cytosine and search for active demethylation intermediates. *PloS One* **2010**, *5* (12), No. e15367.

(7) Ren, Y.; Zhang, Z.; She, Y.; He, Y.; Li, D.; Shi, Y.; He, C.; Yang, Y.; Zhang, W.; Chen, C. A Highly Sensitive and Specific Non -Invasive Test through Genome -Wide 5 -Hydroxy methylation Mapping for Early Detection of Lung Cancer. *Small Methods* **2023**, *8* (3), No. 2300747.

(8) Kriaucionis, S.; Heintz, N. The nuclear DNA base 5-Hydroxymethyl cytosine is present in Purkinje neurons and the brain. *Science* **2009**, *324* (5929), 929−930.

(9) Szulwach, K. E.; Li, X.; Li, Y.; Song, C.-X.; Wu, H.; Dai, Q.; Irier, H.; Upadhyay, A. K.; Gearing, M.; Levey, A. I.; et al. 5-hmC−mediated epigenetic dynamics during postnatal neurodevelopment and aging. *Nat. Neurosci.* **2011**, *14* (12), 1607−1616.

(10) Lee, S. Y.; Qi, X.; Ko, M.; Park, C. H.; An, J.; Lim, S. Direct and rapid detection of 5-hydroxymethylcytosine, a novel cancer hallmark in DNA, using electrochemical reaction. *Mater. Today Commun.* **2020**, *25*, No. 101399.

(11) Zhao, J.; Yan, J.; Li, J.; Shi, G.; Su, M.; Liu, C.; Jia, G. Selective Ligase- Based Sample Processing-Free Discrimination and Detection of Site-Specific DNA 5-Hydroxymethylcytosine. *Anal. Chem.* **2024**, *96* (32), 13285−13290.

(12) Szwagierczak, A.; Bultmann, S.; Schmidt, C. S.; Spada, F.; Leonhardt, H. Sensitive enzymatic quantification of 5-hydroxymethylcytosine in genomic DNA. *Nucleic Acids Res.* **2010**, *38* (19), No. e181.

(13) Ito, S.; D'Alessio, A. C.; Taranova, O. V.; Hong, K.; Sowers, L. C.; Zhang, Y. Role of Tet proteins in 5mC to 5hmC conversion, ES-cell self-renewal and inner cell mass specification. *Nature* **2010**, *466* (7310), 1129−1133.

(14) Koh, K. P.; Yabuuchi, A.; Rao, S.; Huang, Y.; Cunniff, K.; Nardone, J.; Laiho, A.; Tahiliani, M.; Sommer, C. A.; Mostoslavsky, G.; et al. Tet1 and Tet2 regulate 5-hydroxymethylcytosine production and cell lineage specification in mouse embryonic stem cells. *Cell Stem Cell* **2011**, *8* (2), 200−213.

(15) Li, W.; Zhang, X.; Lu, X.; You, L.; Song, Y.; Luo, Z.; Zhang, J.; Nie, J.; Zheng, W.; Xu, D.; et al. 5-Hydroxymethylcytosine signatures in circulating cell-free DNA as diagnostic biomarkers for human cancers. *Cell Res.* **2017**, *27* (10), 1243−1257.

(16) Mahaira, L. G.; Katsara, O.; Pappou, E.; Iliopoulou, E. G.; Fortis, S.; Antsaklis, A.; Fotinopoulos, P.; Baxevanis, C. N.; Papamichail, M.; Perez, S. A. IGF2BP1 expression in human mesenchymal stem cells significantly affects their proliferation and is under the epigenetic control of TET1/2 demethylases. *Stem Cells Dev.* **2014**, *23* (20), 2501−2512.

(17) Shao, J.; Shah, S.; Ganguly, S.; Zu, Y.; He, C.; Li, Z. Cell-free DNA 5- hydroxymethylcytosine is highly sensitive for MRD assessment in acute myeloid leukemia. *Clin. Epigenet.* **2023**, *15* (1), No. 134.

(18) Szulwach, K. E.; Li, X.; Li, Y.; Song, C.-X.; Han, J. W.; Kim, S.; Namburi, S.; Hermetz, K.; Kim, J. J.; Rudd, M. K.; et al. Integrating 5-Hydroxymethyl cytosine into the epigenomic landscape of human embryonic stem cells. *PLoS Genet.* **2011**, *7* (6), No. e1002154.

(19) Wu, H.; D'Alessio, A. C.; Ito, S.; Xia, K.; Wang, Z.; Cui, K.; Zhao, K.; Sun, Y. E.; Zhang, Y. Dual functions of Tet1 in transcriptional regulation in mouse embryonic stem cells. *Nature* **2011**, *473* (7347), 389−393.
(20) Wu, H.; Zhang, Y. Mechanisms and functions of Tet protein-mediated 5- methylcytosine oxidation. *Genes Dev.* **2011**, *25* (23), 2436−2452.
(21) (a) Wu, H.; Zhang, Y. Tet1 and 5-hydroxymethylation: a genome-wide view in mouse embryonic stem cells. *Cell Cycle* **2011**, *10* (15), 2428−2436. (b) Wu, H.; Zhang, Y. Tet1 and 5-hydroxymethylation: a genome-wide view in mouse embryonic stem cells. *Cell Cycle* **2011**, *10* (15), 2428−2436.
(22) Zhou, B.; Magana, L.; Hong, Z.; Huang, L. S.; Chakraborty, S.; Tsukasaki, Y.; Huang, C.; Wang, L.; Di, A.; Ganesh, B.; et al. The angiocrine Rspondin3 instructs interstitial macrophage transition via metabolic − epigenetic reprogramming and resolves inflammatory injury. *Nat. Immunol.* **2020**, *21* (11), 1430−1443.
(23) Tahiliani, M.; Koh, K. P.; Shen, Y.; Pastor, W. A.; Bandukwala, H.; Brudno, Y.; Agarwal, S.; Iyer, L. M.; Liu, D. R.; Aravind, L.; Rao, A. Conversion of 5- methylcytosine to 5-hydroxymethylcytosine in mammalian DNA by MLL partner TET1. *Science* **2009**, *324* (5929), 930−935.
(24) Liutkevičiūtė, Z.; Lukinavičius, G.; Masevičius, V.; Daujotytė, D.; Klimašauskas, S. Cytosine-5-methyltransferases add aldehydes to DNA. *Nat. Chem. Biol.* **2009**, *5* (6), 400−402.
(25) Le, T.; Kim, K.-P.; Fan, G.; Faull, K. F. A sensitive mass spectrometry method for simultaneous quantification of DNA methylation and hydroxy methylation levels in biological samples. *Anal. Biochem.* **2011**, *412* (2), 203−209.
(26) Ding, J.; Zhou, Y.; Wang, Q.; Ai, S. Photoelectrochemical biosensor for DNA hydroxymethylation detection based on the enhanced photoactivity of in- situ synthesized $Bi_4NbO_8Cl@Bi_2S_3$ heterojunction. *Biosens. Bioelectron.* **2021**, *194*, No. 113580.
(27) Song, C. X.; Sun, Y.; Dai, Q.; Lu, X. Y.; Yu, M.; Yang, C. G.; He, C. Detection of 5 -Hydroxymethylcytosine in DNA by Transferring a Keto -Glucose by Using T4 Phage β -Glucosyltransferase. *Chem. Bio Chem.* **2011**, *12* (11), 1682−1685.
(28) Nestor, C. E.; Meehan, R. R. Hydroxymethylated DNA immunoprecipitation (hmeDIP). In Functional analysis of DNA and chromatin. *Springer* **2014**, *1094*, 259−267.
(29) Yu, M.; Hon, G. C.; Szulwach, K. E.; Song, C. X.; Zhang, L.; Kim, A.; Li, X.; Dai, Q.; Shen, Y.; Park, B.; et al. Base-resolution analysis of 5-Hydroxy methylcytosine in the mammalian genome. *Cell* **2012**, *149* (6), 1368−1380.
(30) Booth, M. J.; Ost, T. W.; Beraldi, D.; Bell, N. M.; Branco, M. R.; Reik, W.; Balasubramanian, S. Oxidative bisulfite sequencing of 5-methylcytosine and 5-hydroxymethylcytosine. *Nat. Protoc.* **2013**, *8* (10), 1841−1851.
(31) Hadden, J. M.; Convery, M. A.; Dclais, A.-C.; Lilley, D. M.; Phillips, S. E. Crystal structure of the Holliday junction resolving enzyme T7 endonuclease I. *Nat. Struct. Biol.* **2001**, *8* (1), 62−67.
(32) Mean, R. J.; Pierides, A.; Deltas, C. C.; Koptides, M. Modification of the enzyme mismatch cleavage method using T7 endonuclease I and silverstaining. *BioTechniques* **2004**, *36* (5), 758−760.
(33) Zhang, X.; Yang, L.; Wang, F.; Liu, Z.; Liu, R.; Ying, Q.; Fan, C.; Wu, X. Development of a Simple and Cost-Effective Method Based on T7 Endonuclease Cleavage for Detection of Single Nucleotide Polymorphisms. *Genet. Test. Mol. Biomarkers* **2018**, *22* (12), 719−723.
(34) Pittenger, M. F.; Discher, D. E.; Pault, B. M.; Phinney, D. G.; Hare, J. M.; Caplan, A. I. Mesenchymal stem cell perspective: cell biology to clinical progress. *npj Regener. Med.* **2019**, *4* (1), No. 22.

https://doi.org/10.1021/jacsau.4c01184
JACS Au 2025, 5, 1320−1327